Disulfide Bond Rearrangement during Formation of the Chorionic Gonadotropin β-Subunit Cystine Knot in Vivo†

Jason A. Wilken‡,§ and Elliott Bedows*,‡,§,||

Department of Biochemistry and Molecular Biology, Eppley Institute for Research in Cancer and Allied Diseases and University of Nebraska Medical Center Eppley Cancer Center, Department of Obstetrics and Gynecology and Olson Center for Women's Health, and Department of Pharmacology, University of Nebraska Medical Center, Omaha, Nebraska 68198-3255

Received January 19, 2004; Revised Manuscript Received March 1, 2004

ABSTRACT: The intracellular kinetic folding pathway of the human chorionic gonadotropin β-subunit (hCG-β) reveals the presence of a disulfide between Cys residues 38−57 that is not detected by X-ray analysis of secreted hCG-β. This led us to propose that disulfide rearrangement is an essential feature of cystine knot formation during CG-β folding. To test this, we used disulfide bond formation to monitor progression of intracellular folding intermediates of a previously uncharacterized protein, the CG-β subunit of cynomolgous macaque (*Macaca fascicularis*). Like its human counterpart hCG-β with which it shares 81% identity, macaque (m)CG-β is a cystine knot-containing subunit that assembles with an α-subunit common to all glycoprotein hormone members of its species to form a biologically active heterodimer, mCG, which, like hCG, is required for pregnancy maintenance. An early mCG-β folding intermediate, mpβ1, contained two disulfide bonds, one between Cys34 and Cys88 and the other between Cys38 and Cys57. The subsequent folding intermediate, mpβ2-early, was represented by an ensemble of folding forms that, in addition to the two disulfides mentioned above, included disulfide linkages between Cys9 and Cys57 and between Cys38 and Cys90. These latter two disulfides are those contained within the β-subunit cystine knot and reveal that a disulfide exchange occurred during the mpβ2-early folding step leading to formation of the mCG-β knot. Thus, while defining the intracellular kinetic protein folding pathway of a monkey homologue of CG-β, we detected the previously predicted disulfide exchange event crucial for CG-β cystine knot formation and attainment of CG-β assembly competence.

Chorionic gonadotropin (CG),[1] the placental member of the glycoprotein hormone family of humans and higher primates, is a noncovalently associated heterodimer required for the maintenance of pregnancy in these species (*1*). The β-subunit of CG contains twelve conserved cysteine residues that form six intramolecular disulfide (S−S) bonds, three of which comprise a cystine knot (*2*, *3*). The cystine knot is the defining motif of a large superfamily of proteins including the cystine knot-containing growth factors of which CG is a member (*4*, *5*).

The β-subunit of human CG (hCG-β) was the first mammalian protein whose in vivo folding pathway was defined (*6*, *7*). The intracellular kinetic folding pathway of hCG-β was elucidated using S−S bond formation as an index of folding (*6*−*8*). The described order of S−S bond formation and the conversion of hCG-β folding intermediates is

$$\text{(h)p}\beta\text{1-early} \xrightarrow[38-57]{34-88} \text{(h)p}\beta\text{1-late} \xrightarrow[23-72]{9-90}$$
$$\text{(h)p}\beta\text{2-free} \xrightarrow[+\alpha\text{-subunit}]{93-100} \text{(h)p}\beta\text{2-combined} \xrightarrow{26-110}$$
$$\text{native (h)}\alpha,\beta\text{ dimer} \quad (1)$$

where the numbers above the arrows designate cysteine residues that form S−S linkages as hCG-β folding progresses and the second arrow shows the conversion of the early assembly-incompetent folding intermediate, pβ1, to a second assembly-competent intermediate, pβ2. However, the disulfide assignments of the in vivo folding pathway shown in eq 1 deviate from those detected by X-ray analysis of mature, secreted urinary hCG-β (*2*, *3*).

According to the crystal structure (*2*, *3*) of secreted hCG-β, the pairings of the cysteine residues are Cys9−Cys57, Cys34−Cys88, Cys38−Cys90, Cys23−Cys72, Cys26−Cys110, and Cys93−Cys100, the first three of which comprise a cystine knot motif (*4*, *5*). The respective assignments of hCG-β S−S bonds 34−88, 23−72, 93−100, and 26−110 do not vary between the intracellular folding

† This material is based upon work supported in part by NCI Cancer Center Support Grant P 30 CA36727 and NCI Training Grant CA09746 to the Eppley Institute Cancer Center, a grant from the University of Nebraska Medical Center Olson Center for Women's Health (to E.B.), and an Emley Fellowship (to J.A.W.).

* To whom correspondence should be addressed at the Department of Obstetrics and Gynecology, University of Nebraska Medical Center, 983255 Nebraska Medical Center, Omaha, NE 68198-3255. Tel: 402-559-6074. Fax: 402-559-8112. E-mail: ebedows@unmc.edu.

‡ Department of Biochemistry and Molecular Biology.

§ Eppley Institute for Research in Cancer and Allied Diseases and University of Nebraska Medical Center Eppley Cancer Center.

|| Department of Obstetrics and Gynecology, Olson Center for Women's Health, and Department of Pharmacology.

[1] Abbreviations: BPTI, bovine pancreatic trypsin inhibitor; CG, chorionic gonadotropin; GPH, glycoprotein hormone; C_4 RP-HPLC$_{TFA}$, C_4 reversed-phase column high-pressure liquid chromatography with 0.1% TFA in buffers; C_{18} RP-HPLC$_{PHOS}$, C_{18} reversed-phase column high-pressure liquid chromatography with 10 mM sodium phosphate, pH 7.4, in buffers; C_{18} RP-HPLC$_{TFA}$, C_{18} reversed-phase column high-pressure liquid chromatography with 0.1% TFA in buffers; PAGE, polyacrylamide gel electrophoresis; S−S, disulfide.

10.1021/bi049856x CCC: $27.50
Published on Web 04/07/2004

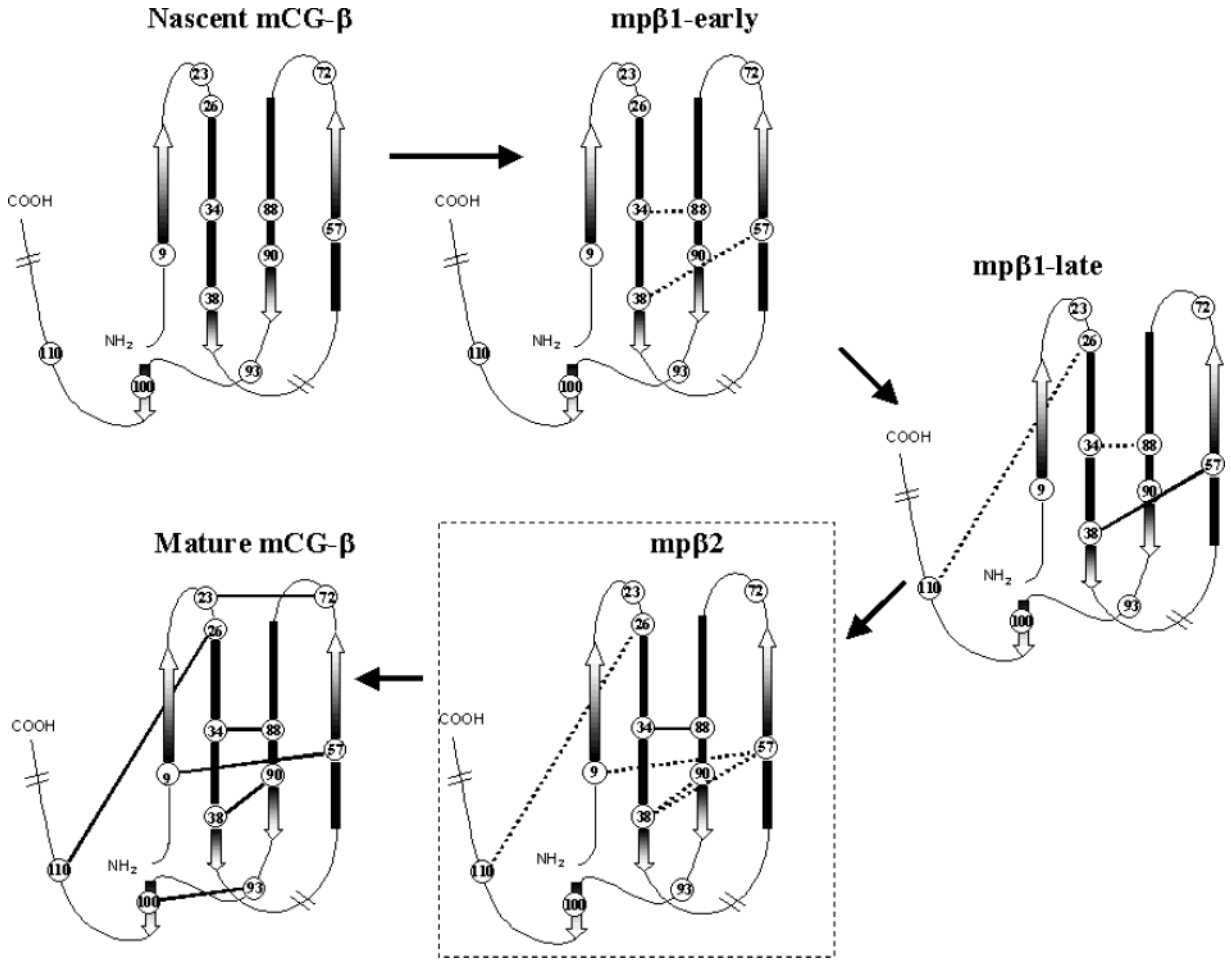

FIGURE 1: Model of the mCG-β intracellular kinetic folding pathway. Shown is our model for the intracellular kinetic folding pathway of mCG-β, determined using disulfide bond formation as an index of folding. The novel ensemble of folding intermediates, collectively termed mpβ2, is depicted in the box. The various S−S-linked folding forms required for S−S bond rearrangement and cystine knot production are indicated (i.e., 9−57, 38−57, and 38−90). Completely formed S−S bonds are depicted with solid lines, while incompletely formed S−S bonds are depicted with broken lines.

assignments and those of secreted hCG-β. However, the existence of S−S bonds 9−57 and 38−90 determined by X-ray analysis is at variance with the assignments of the kinetic folding pathway, which reveals the formation of disulfide 38−57 and the formation of a S−S containing Cys9 and one containing Cys57 forming minutes apart (*9*). This discrepancy implies that a disulfide exchange occurs during, or perhaps after, hCG-β folds.

The reason for the difference in S−S assignments has been resolved in this study by exploiting the fact that a naturally occurring homologue of hCG exists, the CG of the cynomolgous macaque (*Macaca fascicularis*; here termed mCG) (*10*). We have defined the folding pathway of the mCG β1-subunit (GenBank accession number AY026359), which has 81% amino acid identity with hCG-β including all cysteine residues and N-linked glycosylation consensus sequences (*10*), and discovered that although the mCG-β early kinetic folding pathway paralleled that of hCG-β, a novel folding intermediate was detected. This intermediate facilitated identification of the step within the CG-β folding pathway where the S−S exchange, required for cystine knot formation, occurred. As depicted in Figure 1, we have now detected the previously predicted disulfide exchange event (*11*, *12*) crucial for cystine knot formation and the creation of an assembly-competent CG-β subunit.

EXPERIMENTAL PROCEDURES

Cell Culture. 293T cells (*13*) were grown in Dulbecco's modified Eagle's medium (Invitrogen) supplemented with penicillin/streptomycin (100 units/mL and 100 μg/mL, respectively) (Invitrogen) and 10% fetal bovine serum (Atlanta Biologicals). Untransfected CHO cells were grown in F12 HAM media (Invitrogen) supplemented with penicillin/streptomycin and 5% fetal bovine serum. CHO cells stably transfected with mCG-β were grown in Ultraculture (Biowhittaker) supplemented with penicillin/streptomycin and 50 μM methionine sulfoxamine (Sigma).

Transient Transfection of 293T Cells. 293T cells (2×10^6 per dish) were plated into 60 mm plastic dishes and grown to 70−80% confluency overnight. Plasmid DNA was precipitated as described previously (*14*). To ensure uniform precipitation, one large-scale preparation was distributed equally among all dishes. Cells were then incubated for 2 days at 37 °C and used for metabolic labeling.

Stable Transfection of CHO Cells. CHO cells expressing GPH-α (a gift of Dr. Irving Boime, Washington University, St. Louis, MO) were transfected with a plasmid DNA, pGS (*8*), encoding CG-β constructs. Stable clones were selected using the methionine sulfoxamine/glutamate synthetase system (*15*). CG-β expression levels were assayed by silver stain of immunoprecipitated conditioned media.

Metabolic Labeling with [^{35}S]Cysteine. Transiently transfected 293T or stably transfected CHO cells were pulse-labeled with L-[^{35}S]cysteine (~1100 Ci/mmol; PerkinElmer Life Sciences; concentration of 50−150 μCi/mL) in serum-free medium lacking cysteine and chased for the times indicated in the text. Cells were harvested by rinsing one time with cold phosphate-buffered saline followed by immediate lysis in phosphate-buffered saline containing detergents (1.0% Triton X-100, 0.5% sodium deoxycholate, and 0.1% SDS), 2 mM phenylmethanesulfonyl fluoride, and 50 mM iodoacetate, pH 8.3, to trap free thiols in folding intermediates (*6*, *7*).

Immunoprecipitation of Culture Media. Immunoreactive forms of h- and mCG-β were efficiently precipitated with polyclonal antiserum that recognizes all known conformations of hCG-β (*7*). Immunoprecipitations were carried out at 4 °C overnight with rotation in the dark. Immune complexes were precipitated with protein A−Sepharose (Sigma) and prepared for reversed-phase (RP) HPLC as described below.

RP-HPLC Purification of mCG-β Subunits. Radiolabeled CG subunits adsorbed to protein A−Sepharose beads were prepared as described previously (*7*). Briefly, protein A−Sepharose bead/antibody−antigen immunocomplexes were washed three times with phosphate-buffered saline containing detergents (1% Triton X-100, 0.5% sodium deoxycholate, 0.1% SDS) followed by four washes with phosphate-buffered saline lacking detergents. Immunocomplexes were pelleted between washes by centrifugation for 1 min at 2000*g*. To dissociate the Sepharose/antibody−antigen interactions, immunocomplexes were treated with 6 M guanidine hydrochloride, pH 3.0 (sequanal grade; Pierce), overnight with rotation at 22 °C. Myoglobin (100 μg) (Sigma) was added as a carrier. The guanidine eluates were injected onto a Vydac 300 Å C_4 reversed-phase column equilibrated with 0.1% trifluoroacetic acid (C_4 RP-HPLC$_{TFA}$) and eluted using an acetonitrile gradient as described previously (*7*). Fractions were collected in 1 min intervals and quantitated by scintillation counting. Samples were stored at −20 °C for further characterization.

Tryptic Mapping Strategy. The tryptic mapping strategy consisted of three steps. First, [^{35}S]cysteine-containing CG-β was fully reduced and alkylated and then digested with trypsin. The tryptic fragments were separated by HPLC, generating a map of reduced, alkylated peptides. Those HPLC fractions containing cysteine were identified by virtue of their radiolabel and pooled, and the resulting peptides were identified by Edman degradation. In the second step, each mCG-β folding intermediate was individually digested with trypsin without prior reduction and alkylation. HPLC elution profiles of these digests reveal missing fragments and new peaks. By inference, the new peaks represent S−S-linked complexes of the missing fragments. In the third step, the S−S-linked complexes were collected, reduced and alkylated, and individually resubjected to HPLC separation in order to identify the fragments that were S−S-linked.

Step 1. The reduced, alkylated mCG-β tryptic map was created as follows. [^{35}S]Cysteine-containing mCG-β was fully reduced and alkylated by incubation with 5 mg/mL DTT, pH 8, for 3 h at 37 °C, followed by a 20 min alkylation with 50 mM iodoacetate. The reduced and alkylated mCG-β was then digested overnight with 0.03% trypsin in a silanized polypropylene tube also containing 100−200 μg of myoglobin, 5 mM $CaCl_2$, and 100 mM Tris-HCl, pH 8.0. Digestions continued for 2 h with the addition of two 25 μg aliquots of trypsin (0.06% final concentration) for 1 h each. The resulting tryptic peptides were separated on a Vydac C_{18} reversed-phase column as described previously (*7*). Briefly, the column was eluted isocratically for 3 min with 0.1% trifluoroacetic acid, pH 3.0 (C_{18} RP-HPLC$_{TFA}$), or 10 mM sodium phosphate, pH 7.4 (C_{18} RP-HPLC$_{PHOS}$), followed by a 0.32%/min acetonitrile gradient in 0.1% trifluoroacetic acid or 10 mM sodium phosphate, pH 7.4, for 100 min. The flow rate was 1.0 mL/min. Fractions were collected in 1 min intervals and quantitated by scintillation counting. Peptides within [^{35}S]cysteine-containing peaks were identified by automated N-terminal Edman degradation with previously described modifications (*16*) on an Applied Biosystem 477A protein sequencer by the Protein Structure Core Facility, University of Nebraska Medical Center, Omaha, NE. Fractions were collected for 10 cycles, and the resulting eluates were quantitated by scintillation counting.

Step 2. Isolated mCG-β folding intermediates were pooled, concentrated, and digested with trypsin (as described above) without prior reduction and alkylation. The digested intermediates were then subjected to C_{18} RP-HPLC$_{TFA}$, and the elution profiles of these digests were compared to the mCG-β reduced and alkylated tryptic map to reveal missing fragments and new peaks. The new peaks were rechromatographed by C_{18} RP-HPLC$_{PHOS}$ to identify free peptides that might have coeluted by C_{18} RP-HPLC$_{TFA}$.

Step 3. The newly identified peaks were individually collected, reduced and alkylated, and resubjected to the C_{18} RP-HPLC$_{TFA}$ separation to identify the S−S-linked fragments. When multiple peptides were recovered from a single peak, S−S linkages were assigned on the basis of S−S bonds previously detected in CG-β by X-ray crystallography (*2*, *3*) or kinetic analysis (*9*). Additionally, ion-exchange chromatography as previously described (*6*, *7*) was used to confirm S−S assignments.

RESULTS

Identification of mCG-β Folding Intermediates by HPLC. The earliest major intracellular folding intermediate of wild-type hCG-β, pβ1, is readily detected as a diffuse band that migrates with M_r = 23 000 by SDS−PAGE under non-reducing conditions (*6*−*8*). However, the pβ1 folding intermediate of human LH-β (*17*) and that of the naturally occurring hCG-βV79M variant (*18*) cannot be detected by this assay. This is because there is a great deal of conformational variation in the early forms of hLH-pβ1 and hCG-βV79M pβ1, so the respective pβ1 forms spread throughout a nonreducing SDS-containing gel making identification of individual conformers difficult using this technique. That these pβ1 conformers are efficiently precipitated by our polyclonal antiserum against hCG-β has been demonstrated. We can quantitatively detect either of these pβ1 forms by SDS−PAGE under reducing conditions (which eliminates conformational variation) as well as by C_4 RP-HPLC$_{TFA}$ (*17*, *18*). Similarly, the pβ1 folding intermediate of mCG-β could not be detected efficiently by nonreducing SDS−PAGE because of its great conformational variability but was efficiently detected by C_4 RP-HPLC$_{TFA}$. Thus, we used C_4

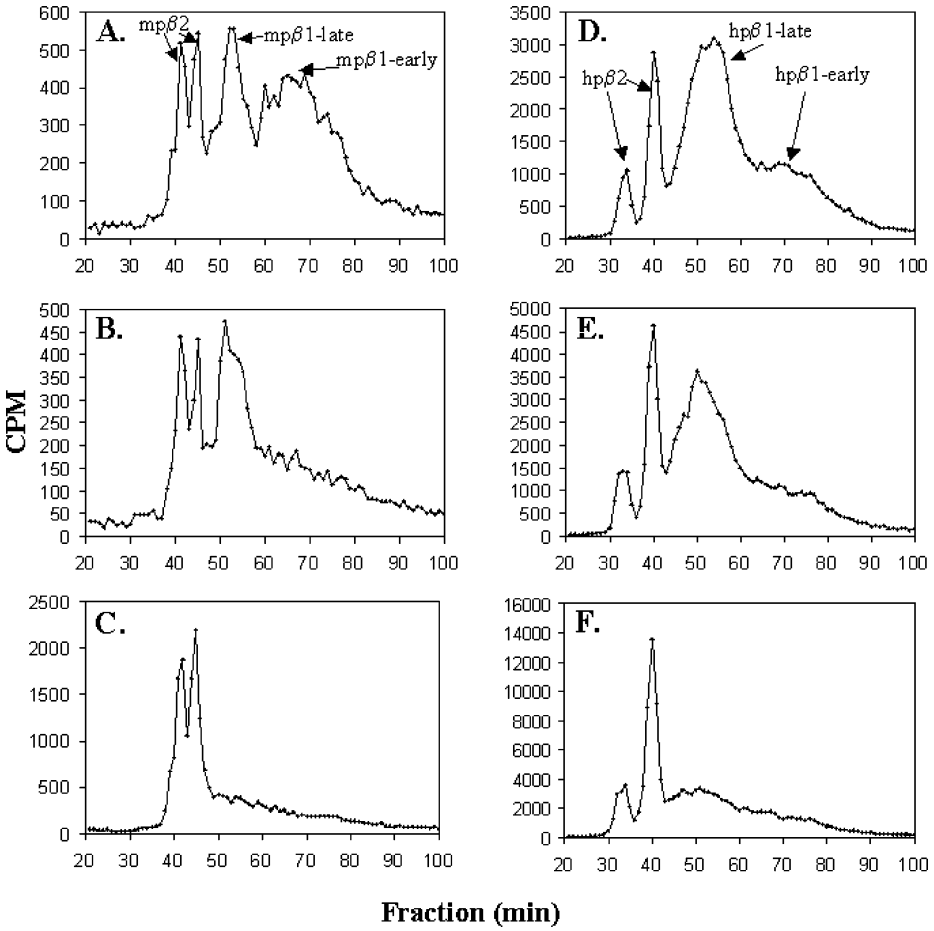

FIGURE 2: Kinetics of mCG-β folding. Confluent cultures of 293T cells transiently transfected with plasmids encoding either mCG-β (panels A−C) or hCG-β (panels D−F) genes were pulse labeled for 5 min with [^{35}S]Cys and chased for 0 min (panels A and D), 5 min (panels B and E), or 15 min (panels C and F). The panels show the C_4 RP-HPLC$_{TFA}$ elution profiles, CPM vs fraction, where the fractions were collected at 1 min intervals. Folding intermediates m or h pβ1-early, pβ1-late, and pβ2 are indicated.

RP-HPLC$_{TFA}$, rather than SDS−PAGE, to study the precursor−product relationships during mCG-β folding (Figure 2).

As previously described (*6*−*8*, *12*), hCG-β folds through a series of distinct S−S bond-containing intermediates (see eq 1), and its folding pathway is independent of cell type used (*6*, *7*, *18*, *19*). Similarly, there were no differences in mCG-β folding kinetics or the folding intermediates when CHO cells were stably transfected with mCG-β or 293T cells transiently transfected with plasmids expressing mCG-β (data not shown). The earliest detectable intracellular mCG-β folding intermediate, mpβ1-early (see Figure 2), eluted as a broad peak at about 65 min, while a subsequent folding intermediate, mpβ1-late, also eluted as a broad peak at about 52 min. A late folding intermediate, mpβ2, eluted as a doublet at 41 and 45 min.

Panels A−C of Figure 2 show the precursor−product relationship between these mCG-β intracellular folding forms. The three distinct mCG-β folding intermediates were detected following a 5 min pulse labeling with [^{35}S]Cys and 0 min chase (Figure 2A). After a 5 min chase (Figure 2B), mpβ1-early was mostly converted to mpβ1-late. After a 15 min chase (Figure 2C), nearly all of the mpβ1-late had converted to mpβ2. Similar folding kinetics were observed for hCG-β, after a 0 min chase (Figure 2D), 5 min chase (Figure 2E), and 15 min chase (Figure 2F). Thus, progression of mCG-β folding intermediates paralleled those of hCG-β (Figure 2D−F), except that a greater percentage of the earliest mCG-β folding intermediate, mpβ1-early, was recovered compared to the equivalent hCG-β folding intermediate, hpβ1-early (compare panels A−D of Figure 2). To analyze the S−S nature of mCG-β folding intermediates, RP-HPLC tryptic mapping was performed at two different pHs as described below.

Generation of a Reduced, Alkylated mCG-β Tryptic Map. RP-HPLC using 0.1% trifluoroacetic acid, pH 3, as coupling agent (C_{18} RP-HPLC$_{TFA}$) has been previously used to isolate and identify tryptic peptides of hCG-β (*6*, *7*). Here, we used a similar strategy to generate a reduced, alkylated mCG-β tryptic map by identifying and sequencing Cys-containing mCG-β peptides generated following trypsin digestion of mCG-β, as described in step 1 of Tryptic Mapping Strategy in Experimental Procedures. As summarized in Table 1 and shown in Figure 3A, mCG-β tryptic peptides eluted as follows: peptide 96−104, representing reduced thiol Cys100, eluted as a doublet at min 8 and min 20 (peaks 1a and 1b); peptide 90−94, representing reduced thiols Cys90 and Cys93, eluted at min 35 (peak 2); peptide 105−122, representing reduced thiol Cys110, eluted at min 48 (peak 3); peptide 9−20, representing reduced thiol Cys9, eluted at min 51 (peak 4); peptide 21−43, representing reduced thiols Cys23, Cys26, Cys34, and Cys38, eluted at min 75 (peak 5); peptide 69−89, representing reduced thiols Cys72 and Cys88, eluted at min 93 (peak 6); and peptide 44−60, representing reduced thiol Cys57, eluted at min 98 (peak 7).

Table 1: Identification of mCG-β Tryptic Peptides

peak	tryptic peptide	unbound cysteine residues	elution fraction (min) C_{18} RP-$HPLC_{TFA}$	elution fraction (min) C_{18} RP-$HPLC_{PHOS}$
1a, 1b	96−104	Cys100	8, 20	
2	90−94	Cys90, Cys93	35	
3	105−122	Cys110	48	
4	9−20	Cys9	51	
5	21−43	Cys23, Cys26, Cys34, Cys38	75	44
6	69−89	Cys72, Cys88	93	64
7	44−60	Cys57	98	94

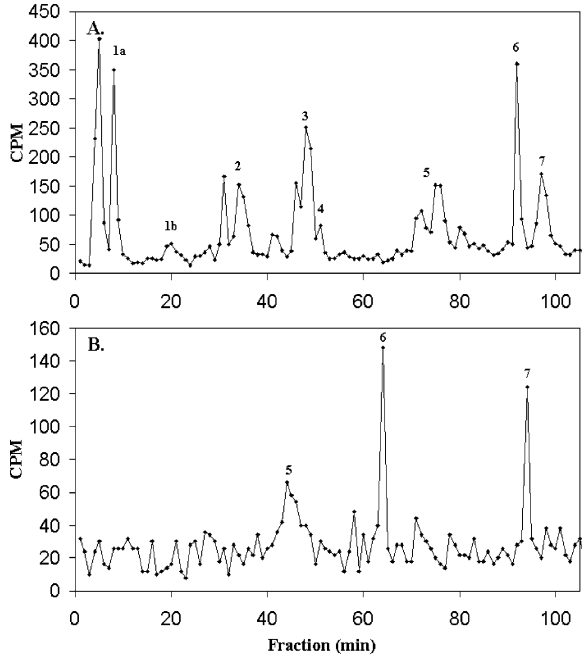

FIGURE 3: Identification of mCG-β tryptic peptides. To perform tryptic analysis of mCG-β folding intermediates, the elution positions of mCG-β tryptic peptides were determined by treatment of [^{35}S]Cys-labeled mCG-β with dithiothreitol followed by alkylation of free thiols with iodoacetate and trypsin digestion (*6*, *7*). Panels: A, tryptic peptides of mCG-β separated by C_{18} RP-$HPLC_{TFA}$; B, tryptic peptides of mCG-β separated by C_{18} RP-$HPLC_{PHOS}$. The identities of the peptides were determined by microsequencing (*15*) and are summarized in Table 1.

Three peaks (peaks 5, 6, and 7), containing peptides 21−43, 69−89, and 44−60, respectively, which eluted at 75, 93, and 98 min, were reanalyzed by C_{18} RP-$HPLC_{PHOS}$ (Figure 3B) as described in Experimental Procedures. This was required because these peptides coeluted with S−S-linked complexes from unreduced tryptic digests in a 0.1% TFA-containing buffer (see below); use of C_{18} RP-$HPLC_{PHOS}$ at pH 7.4, rather than C_{18} RP-$HPLC_{TFA}$ at pH 3, provided an alternative tryptic map that altered the respective peptide elution times and facilitated their identification. Using C_{18} RP-$HPLC_{PHOS}$ analysis, mCG-β peptide 21−43 (peak 5) eluted at 44 min rather than 75 min, peptide 69−89 (peak 6) eluted at 64 min rather than at 93 min, and peptide 44−60 (peak 7) eluted at 94 min rather than at 98 min [see Figure 3B (compare to equivalent peaks in Figure 3A) and Table 1].

Tryptic Analysis of mCG-β Folding Intermediates. The S−S bond content of nonreduced mCG-β folding intermediates mpβ1-early, mpβ1-late, and mpβ2 was analyzed by tryptic analysis. [^{35}S]Cys-labeled folding intermediates were isolated, pooled, concentrated, and digested with trypsin as described in Experimental Procedures and intermediates analyzed as indicated below. The mCG-β reduced, alkylated tryptic maps shown in Figure 3 were used for comparison.

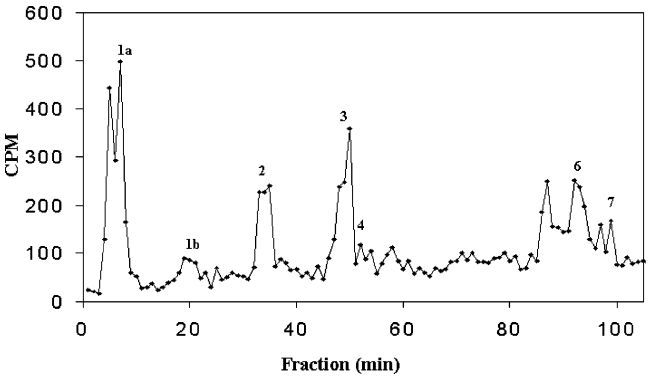

FIGURE 4: Tryptic analysis of mpβ1-early. The tryptic map of nonreduced mpβ1-early was generated by C_{18} RP-$HPLC_{TFA}$ chromatography demonstrating that S−S bonds 34−88 and 38−57 were formed in this early folding intermediate, as described in the text.

(A) mpβ1-early. The nonreduced tryptic map of mpβ1-early is shown in Figure 4. Free peptides were identified by comparison with the mCG-β reduced, alkylated tryptic map (Figure 3 A). Non-S−S-linked peptides 96−104 (peak 1), 90−94 (peak 2), 105−122 (peak 3), and 9−20 (peak 4), representing free thiols Cys100, Cys90 and Cys93, Cys110, and Cys9, respectively, were detected in the nonreduced mpβ1-early tryptic map at levels proportional to that of reduced mCG-β (Figure 3A), indicating that S−S bonds 9−57, 38−90, 93−100, and 26−110 were unformed. Peptides 69−89 (peak 6) and 44−60 (peak 7), representing free thiols Cys88 and Cys57, respectively, were also detected, but in much smaller proportions than when compared to reduced mCG-β, indicating that S−S bonds containing these thiols were formed in part. In addition, peptide 21−43 (peak 5) is not detectable as a free peptide. Although reduction, alkylation, and analysis of mpβ1-early tryptic peaks was not feasible due to the small amount of recovered mpβ1-early, the mpβ1-early tryptic map indicates that, as with hCG-β (*9*), mCG-β S−S bonds 34−88 and 38−57, but no other disulfides, were detected as partially formed in the mpβ1-early folding intermediate.

(B) mpβ1-late. Tryptic analysis of nonreduced mpβ1-late is shown in Figure 5A. Peaks 1, 2, 3, and 4, representing peptides 96−104, 90−94, 105−122, and 9−20, containing thiols Cys100, Cys90 and Cys93, Cys110, and Cys9, respectively, were detected in the nonreduced mpβ1-late tryptic map. However, peaks 1, 3, and 4 are found in lower proportion than in mpβ1-early, indicating that the thiols Cys9, Cys100, and Cys110 were partially S−S bound. Peak 2 of mpβ1-late was found in similar proportion to mpβ1-early, indicating that thiols Cys90 and Cys93 were not S−S bound in mpβ1-late. Late-eluting material at min 69, 86, 91, and 98 in the mpβ1-late map, termed C1, C2, C3, and C4 in Figure 5A, was not detected in mpβ1-early, further suggesting that additional S−S bond formation occurred as mpβ1-early converted to mpβ1-late.

Non-S−S-linked peaks 5, 6, and 7, representing peptides 21−43, 69−89, and 44−60, coeluted with S−S-linked material in C1, C3, and C4, respectively. To resolve non-

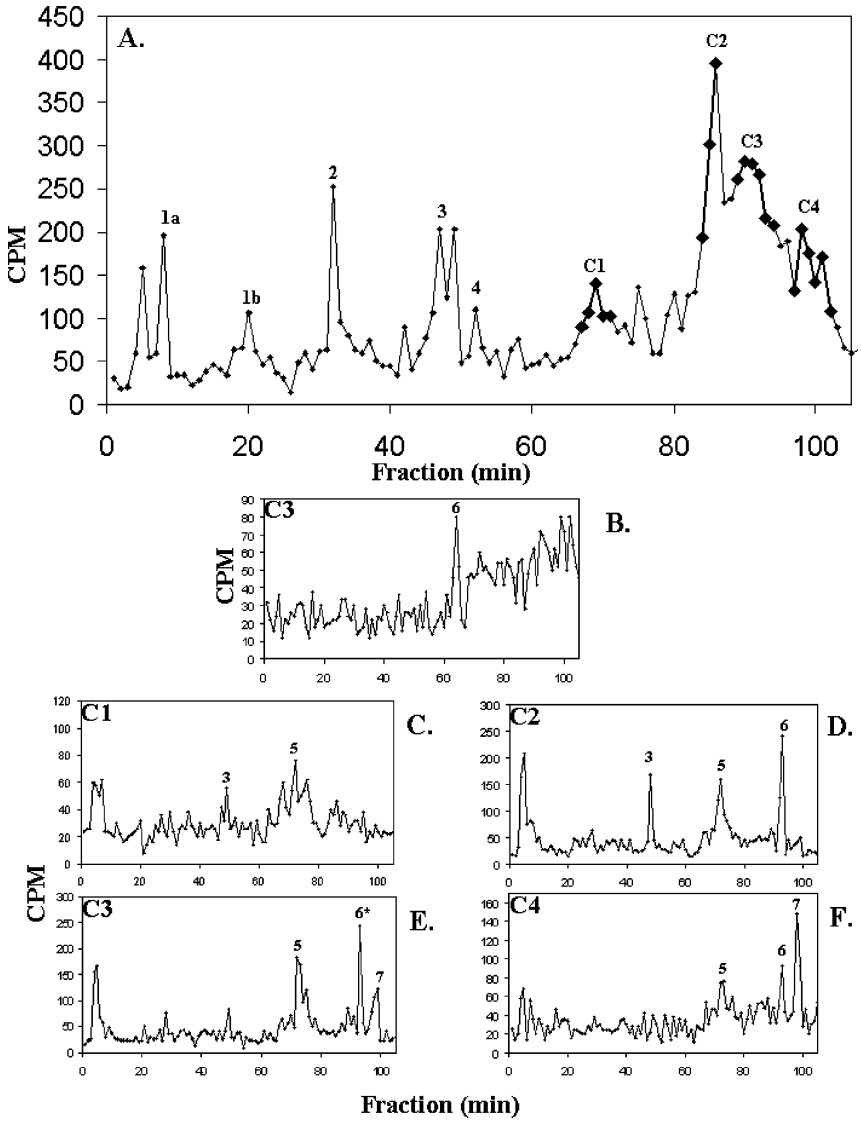

FIGURE 5: Tryptic analysis of mpβ1-late. Panels: A, the nonreducing tryptic map of mpβ1-late generated by C_{18} RP-HPLC$_{TFA}$ as described in the text; B, C_{18} RP-HPLC$_{PHOS}$ of nonreduced peak 6 (peptide 69−89) demonstrating that this peptide was not completely S−S-linked in the mpβ1-late folding intermediate; C−F, C_{18} RP-HPLC$_{TFA}$ of S−S-linked fractions C1, C2, C3, and C4, respectively, following reduction of each, demonstrating which peptides contained S−S bonds (see Table 1). (* = peak 6 was also detected as free peptide in fraction C3 by C_{18}RP-HPLC$_{PHOS}$.)

S−S-linked peptides from S−S-linked material, we chromatographed the material eluting between 70 and 100 min by C_{18} RP-HPLC$_{PHOS}$. When aliquots of material contained within fractions C1 through C4 were analyzed by C_{18} RP-HPLC$_{PHOS}$, peak 6, representing peptide 69−89, was identified as a free peptide within C3 (Figure 5B), but peaks 5 and 7, representing peptides 21−43 and 44−60, were not detected as free peptides in C1 and C3, respectively (data not shown). This demonstrates that S−S bond 34−88, detected in reduced C2 and C4 (see below), is not completely formed in mpβ1-late.

Aliquots of fractions C1, C2, C3, and C4 were then reduced, alkylated, and chromatographed by C_{18} RP-HPLC$_{TFA}$ as described in Experimental Procedures. The elution profile of reduced C1 (Figure 5C) demonstrated that peaks 3 and 5, representing peptides 105−122 and 21−43, containing thiols at Cys110 and Cys23, Cys26, Cys34, and Cys38, respectively, were S−S bound. Based on S−S assignments by previous kinetic and crystallographic studies (*2*, *3*, *6*, *7*, *9*), detection of peptides 105−122 and 21−43 implies partial formation of S−S bond 26−110.

The elution profile of reduced C2 (Figure 5D) demonstrated that peaks 3, 5, and 6, representing peptides 105−122, 21−43, and 69−89, containing thiols Cys110, Cys23, Cys26, Cys34, Cys38, and Cys88, respectively, were S−S bound. The presence of peptides 105−122, 21−43, and 69−89 within a single peak suggests the existence of S−S bonds 34−88 and 26−110.

The elution profile of reduced fraction C3 (Figure 5E) demonstrates that peaks 5 and 7, representing peptides 21−43 and 44−60, were S−S bound, demonstrating the formation of S−S bond 38−57. Peptide 69−89 (peak 6) was detected as a free peptide in peak nonreduced C3 (Figure 5B).

Finally, the elution profile of reduced fraction C4 (Figure 5F) demonstrates that peaks 5, 6, and 7, representing peptides 21−43, 69−89, and 44−60, respectively, were S−S bound, demonstrating the existence of S−S bonds 34−88 and 38−

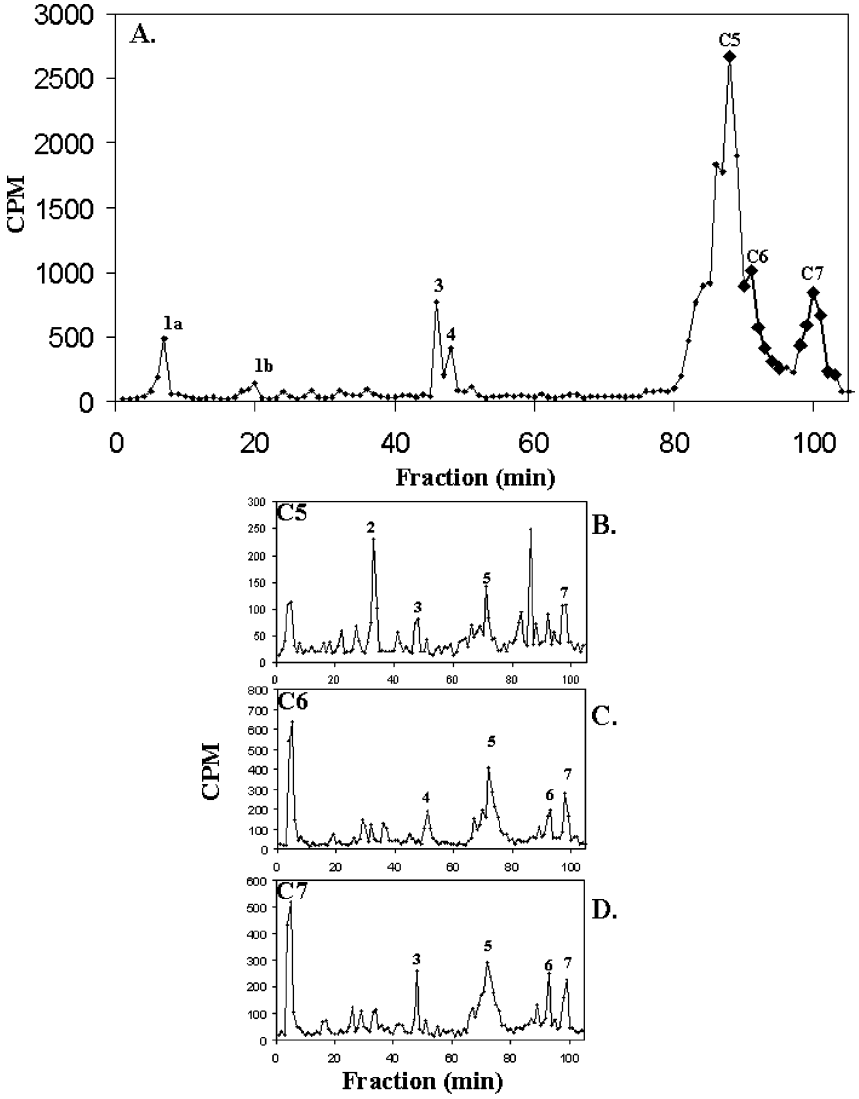

FIGURE 6: Tryptic analysis of mpβ2. Panels: A, the C_{18} RP-HPLC$_{TFA}$-generated tryptic map of nonreduced mpβ2; B−D, C_{18} RP-HPLC$_{TFA}$ of S−S-linked fractions C5, C6, and C7, respectively, following reduction of each, demonstrating which peptides contained S−S bonds (see Table 1).

57. Together, these data reveal that although S−S bonds 34−88, 38−57, and 26−110 were detected in the mpβ1-late folding intermediate, S−S bonds 34−88 and 26−110 were incompletely formed because peptides 105−122 (containing Cys 110) and 69−89 (containing Cys 88) were found in both free and S−S-linked material.

(C) mpβ2. A C_{18} RP-HPLC$_{TFA}$-generated tryptic map of nonreduced mpβ2 is shown in Figure 6A. Peaks 1, 3, and 4, representing peptides 96−104, 105−122, and 9−20, containing free thiols 100, 110, and 9, respectively, were again detected but in lower proportions than in mpβ1-late. The majority of recovered counts were in the form of late-eluting fractions at min 88, 91, and 100 (Figure 6A, fractions, C5, C6, and C7, respectively). Peaks 6, and 7, which normally migrate to this area, failed to be detected by C_{18} RP-HPLC$_{PHOS}$ (data not shown), indicating that the thiols of peptides 69−89 (i.e., Cys88) and 44−60 (i.e., Cys57) are S−S-linked in mpβ2. Aliquots of fractions C5, C6, and C7 were then concentrated, reduced, alkylated, and analyzed by C_{18} RP-HPLC$_{TFA}$. The elution profile of reduced fraction C5 (Figure 6B) revealed that thiols contained within peak 2 (peptide 90−94), peak 3 (peptide 105−122), peak 5 (peptide 21−43), and peak 7 (peptide 44−60) were S−S bound. Therefore, disulfide-linked peptides containing S−S bonds 26−110, 38−90, and 38−57, but not 9−57, were detected in fraction C5.

The elution profile of reduced fraction C6 (Figure 6C) demonstrates that thiols contained within peak 4 (peptide 9−20), peak 5 (peptide 21−43), peak 6 (peptide 69−89), and peak 7 (peptide 44−60) were S−S bound. The presence of peptide 9−20, containing thiol Cys9, as a S−S-linked peptide implies the existence of S−S bond 9−57 in C6, while the presence of peptides 21−43 and 69−89 implies complete formation of S−S bond 34−88.

The elution profile of reduced fraction C7 (Figure 6D) demonstrates that thiols contained within peak 3 (peptide 105−122), peak 5 (peptide 21−43), peak 6 (peptide 69−89), and peak 7 (peptide 44−60) were S−S bound, as well. The presence of peptide 21−43 and both 69−89 and 105−122 indicates the existence of S−S bonds 26−110 and 34−88. The presence of peptides 21−43 and 44−60, but *not* 9−20 or 90−94, as S−S-linked in fraction C7 implies the existence of S−S bond 38−57 and not 9−57 or 38−90 in C7. Taken together, these data indicate that S−S bonds

9−57, 26−110, 34−88, 38−57, and 38−90 were all detected in various fractions of the ensemble of folding intermediates termed mpβ2. The simultaneous existence of S−S bonds 9−57, 38−57, and 38−90 in separate mpβ2 fractions implies that none of the three bonds were fully formed and that a S−S exchange from 38−57 to 9−57 and 38−90 occurred at the mpβ2 step of the CG-β intracellular kinetic folding pathway.

DISCUSSION

CG is a member of the cystine knot-containing family of growth factors. It shares extensive three-dimensional structural similarity with other members of this growth factor superfamily, including PDGF, NGF, TGF-β (*2*) and VEGF (*20*), despite having little amino acid sequence similarity other than the consensus sequences of their respective cystine knot motifs. Here, we determined how this vital motif forms in the β-subunit of CG, a glycoprotein hormone necessary for the maintenance of pregnancy in humans and higher primates (*1*). In hCG-β, the cystine knot S−S bonds 34−88 and 38−90 create an eight amino acid ring structure by bridging adjacent polypeptide segments (residues 34−38 and 88−90) through which S−S bond 9−57 penetrates (*2, 3*). As alluded to above and described in detail below, while previous kinetic studies demonstrate the existence of a S−S linkage between Cys38 and Cys57 in the earliest detectable hCG-β folding intermediate, pβ1 (*9*), no such S−S bond has been identified by X-ray analysis of secreted hCG-β (*2, 3*).

Our objective in this study was to test our prediction that the difference in S−S assignments between the kinetic folding pathway of CG-β and X-ray crystallography of secreted CG-β was due to a S−S rearrangement during the folding or assembly of CG. This was accomplished by defining the intracellular folding pathway of mCG-β, the macaque homologue of hCG-β, during the transition from the early assembly-incompetent folding intermediate, pβ1, to its assembly-competent conformation, pβ2. This involves the formation of the CG-β cystine knot. The rationale for this hypothesis is based not only on the detection of S−S bond 38−57 in early folding intermediates and disulfides 9−57 and 38−90 in secreted hCG-β (*2, 6*), but that the $t_{1/2}$ of detection of a disulfide containing Cys9 and one containing Cys57 are minutes apart [$t_{1/2}$ of formation = 4−5 min for Cys9 and 2−3 min for Cys57 (*9*)]. This implies that the initial S−S linkage containing Cys57 is bound to a thiol other than Cys9 [i.e., Cys38 (*12*)].

Previously (*12*), we reported that it was likely that this S−S exchange occurred as the CG-β assembly-incompetent folding intermediate, pβ1, underwent its major conformational alteration to become assembly-competent pβ2. This assumption was based on the following experimental observations. Replacement of any of the Cys pairs of the knot by Ala or Ser, or a similar substitution of any individual Cys residue of the knot with Ala or Ser, disrupts conversion of assembly-incompetent hpβ1 to assembly-competent hpβ2 (*8, 21*). But removal of any of the non-cystine knot disulfides of hCG-β or a substitution of any individual Cys residue not contained within the cystine knot does not inhibit conversion of pβ1 to pβ2 (*8, 21*). Additionally, molecular chaperone complexes that facilitate the folding of hCG-β subunits lacking both N-linked glycans cannot rescue misfolded unglycosylated hCG-β subunits unless all six Cys residues of the cystine knot are present (*22, 23*). Taken together, these data indicate that the formation of the cystine knot is the rate-limiting step in hCG-β folding and that folding of the subunit into an assembly-competent conformation will not occur without rearrangement of the pβ1 S−S bond 38−57 to disulfides 9−57 and 38−90.

But until now, no direct evidence for that S−S exchange has been reported. Detection of distinct mCG-β folding intermediates containing S−S bridges between Cys residues 38−57, 9−57, and 38−90 (in addition to 34−88) identifies the early pβ2 folding intermediate as the point in the intracellular CG kinetic folding pathway where the predicted S−S exchange occurs, however.

The first mCG-β S−S bonds to form were detected in the mpβ1-early intermediate: S−S bonds 38−57 and 34−88. This is in agreement with findings by Huth et al. (*9*), in which bonds 34−88 and 38−57 begin to form in hpβ1-early. The transition of mpβ1-early to mpβ1-late involved further formation of S−S bond 38−57, as well as the partial formation of S−S bond 26−110. This is also consistent with observations of Huth et al. (*9*). It is likely that the small amount of 26−110 detected in early folding intermediates is transient in nature, since the 26−110 disulfide forms the seat belt that stabilizes the α,β heterodimer and has been shown to be the last bond to complete its formation (*2, 9*).

However, because S−S bond 38−57 is not found in the final structure of CG-β, we must ask what the significance of this S−S bond is in the folding of the CG-β subunit. The role of the 38−57 disulfide may be to bring CG-β loops 1 and 3 (*24, 25*) into proximity so that subsequent folding events, including a disulfide exchange, can occur. This would be consistent with the idea that CG-β S−S rearrangement is a thermodynamic event within the kinetic CG-β folding pathway; the S−S bonds of the cystine knot appear to form and break and re-form in search of a free energy minimum. Once the free energy minimum is attained, orderly formation of all remaining S−S bonds can occur (tryptic analysis of mature, secreted mCG-β shows no free Cys-containing peptides; data not shown). The same is true of hCG-β (*8, 9*).

A comparison of the significance of the in vivo S−S rearrangement events described here for CG-β to classical in vitro studies where S−S rearrangement has been documented reveals interesting parallels. The most extensively studied in vitro folding pathway using S−S bond formation as an index of folding is that of bovine pancreatic trypsin inhibitor (BPTI; *26, 27*). These studies reveal that the in vitro folding of BPTI, whose native disulfide composition is between Cys residues 30−51, 5−55, and 14−38, nonetheless progresses through intermediates containing non-native S−S 5−14 and 5−38. This implies that non-native interactions driven by hydrophobic collapse and hydrogen bond formation are required for BPTI to assume its native conformation in vitro (*28*). However, taken together, these studies reveal that there is, in fact, no efficient pathway by which BPTI folds in vitro. When the folding intermediates that contained non-native S−S 5−14 and 5−38 were purified and allowed to continue to fold, a nonproductive dead-end intermediate formed as readily as did the productive intermediate containing S−S 30−51 and 5−55. These results imply that BPTI employs a more efficient folding pathway in vivo than in vitro. When the in vitro folding of hCG-β was compared to

that of the intracellular folding of the β-subunit (*19*), it was discovered that the same folding intermediates were detected along the kinetic folding pathway, but like the BPTI studies alluded to above, the efficiency of folding of hCG-β was dramatically enhanced in vivo, or even by the addition of protein disulfide isomerase to in vitro reactions (*19*). Thus, while the exact roles of hydrophobic collapse and hydrogen bond formation in S−S bond formation likely vary between proteins, it nonetheless appears that components of the cellular environment facilitate S−S bond formation in particular and protein folding in general (*29*).

Using S−S bond formation as an index of folding the intracellular CG-β folding pathway may now be defined as shown in Figure 1 and the equation:

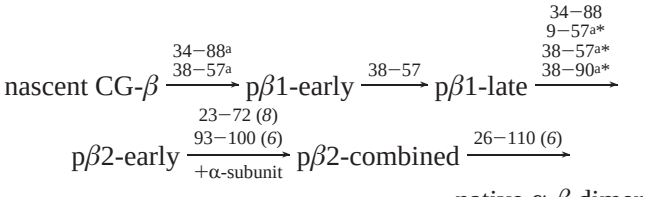

where the numbers over the arrows indicate the S−S bonds that form ("a" indicates the partial formation of a S−S) as mCG-β folding progresses and the asterisks indicate the bonds that are detected during S−S bond exchange, leading to the formation of the CG-β cystine knot. mpβ1-late contains the S−S bond 38−57, which appears to bring other cysteine residues involved cystine knot formation (i.e., Cys9, Cys34, Cys88, and Cys90) into proximity. This proximity would allow for efficient formation and rearrangement of S−S bonds of the cystine knot, including the disruption of 38−57 itself. In this way, S−S bond 38−57 could facilitate its own rearrangement to S−S bonds 9−57 and 38−90 and serve to complete the formation of the β-subunit cystine knot.

In summary, while defining the novel intracellular kinetic folding pathway of mCG-β, we were able to resolve the discrepancies between the disulfide assignments reported during the folding of hCG-β and those seen in secreted CG. Although the mCG-β and hCG-β intracellular pathways are essentially parallel, minor differences in the amino acid composition of mCG-β compared to that of hCG-β altered the kinetics of the folding enough that a novel folding intermediate, mpβ2, was detected. Within the mpβ2 folding intermediate, an ensemble of folding forms of CG-β was identified. This ensemble included all of the S−S bonds predicted to occur during a S−S rearrangement and formation of the CG-β cystine knot. A critical transient disulfide, the S−S bond 38−57 appears in an earlier folding intermediate, pβ1-late. The 38−57 disulfide appears to play a pivotal role in stabilizing this partially folded form of CG-β, facilitating its own rearrangement and allowing cystine knot formation to occur.

ACKNOWLEDGMENT

The authors thank Drs. Ryan J. Darling and Lawrence M. Schopfer for critical review of the manuscript.

REFERENCES

1. Pierce, J. G., and Parsons, T. F. (1981) Glycoprotein hormones: structure and function, *Annu. Rev. Biochem. 50*, 465−495.
2. Lapthorn, A. J., Harris, D. C., Littlejohn, A., Lustbader, J. W., Canfield, R. E., Machin, K. J., Morgan, F. J., and Isaacs, N. W. (1994) Crystal structure of human chorionic gonadotropin, *Nature 369*, 455−461.
3. Wu, H., Lustbader, J. W., Liu, Y., Canfield, R. E., and Hendrickson, W. A. (1994) Structure of human chorionic gonadotropin at 2.6 A resolution from MAD analysis of the selenomethionyl protein, *Structure 2*, 545−558.
4. Isaacs, N. W. (1995) Cystine knots, *Curr. Opin. Struct. Biol. 5*, 391−395.
5. Sun, P. D., and Davies, D. R. (1995) The cystine-knot growth-factor superfamily, *Annu. Rev. Biophys. Biomol. Struct. 24*, 269−291.
6. Huth, J. R., Mountjoy, K., Perini, F., and Ruddon, R. W. (1992) Intracellular folding pathway of human chorionic gonadotropin beta subunit, *J. Biol. Chem. 267*, 8870−8879.
7. Bedows, E., Huth, J. R., and Ruddon, R. W. (1992) Kinetics of folding and assembly of the human chorionic gonadotropin beta subunit in transfected Chinese hamster ovary cells, *J. Biol. Chem. 267*, 8880−8886.
8. Bedows, E., Huth, J. R., Suganuma, N., Bartels, C. F., Boime, I., and Ruddon, R. W. (1993) Disulfide bond mutations affect the folding of the human chorionic gonadotropin-beta subunit in transfected Chinese hamster ovary cells, *J. Biol. Chem. 268*, 11655−11662.
9. Huth, J. R., Mountjoy, K., Perini, F., Bedows, E., and Ruddon, R. W. (1992) Domain-dependent protein folding is indicated by the intracellular kinetics of disulfide bond formation of human chorionic gonadotropin beta subunit, *J. Biol. Chem. 267*, 21396−21403.
10. Wilken, J. A., Matsumoto, K., Laughlin, L. S., Lasley, B. L., and Bedows, E. (2002) Comparison of chorionic gonadotropin expression in human and macaque (Macaca fascicularis) trophoblasts, *Am. J. Primatol. 56*, 89−97.
11. Bedows, E. (2002) Chorionic gonadotropin: Structure−activity relationships of a cystine knot-containing hormone, *Recent Res. Dev. Endocrinol. 3*, 235−247.
12. Bedows, E., Darling, R. J., Wilken, J. A., and Sherman, S. A. (2002) Role of disulphide bond formation in folding, secretion, and assembly of human chorionic gonadotropin subunits, *Indian J. Exp. Biol. 40*, 467−476.
13. Pear, W. S., Nolan, G. P., Scott, M. L., and Baltimore, D. (1993) Production of high-titer helper-free retroviruses by transient transfection, *Proc. Natl. Acad. Sci. U.S.A. 90*, 8392−8396.
14. Darling, R. J., Ruddon, R. W., Perini, F., and Bedows, E. (2000) Cystine knot mutations affect the folding of the glycoprotein hormone alpha-subunit. Differential secretion and assembly of partially folded intermediates, *J. Biol. Chem. 275*, 15413−15421.
15. Lockridge, O., Blong, R. M., Masson, P., Froment, M. T., Millard, C. B., and Broomfield, C. A. (1997) A single amino acid substitution, Gly117His, confers phosphotriesterase (organophosphorus acid anhydride hydrolase) activity on human butyrylcholinesterase, *Biochemistry 36*, 786−795.
16. Steinke, L., and Cook, R. G. (2003) Identification of Phosphorylation Sites by Edman Degradation, *Methods Mol. Biol. 211*, 301−307.
17. Muyan, M., Ruddon, R. W., Norton, S. E., Boime, I., and Bedows, E. (1998) Dissociation of early folding events from assembly of the human lutropin beta-subunit, *Mol. Endocrinol. 12*, 1640−1649.
18. Miller-Lindholm, A. K., Bedows, E., Bartels, C. F., Ramey, J., Maclin, V., and Ruddon, R. W. (1999) A naturally occurring genetic variant in the human chorionic gonadotropin-beta gene 5 is assembly inefficient, *Endocrinology 140*, 3496−3506.
19. Huth, J. R., Perini, F., Lockridge, O., Bedows, E., and Ruddon, R. W. (1993) Protein folding and assembly in vitro parallel intracellular folding and assembly. Catalysis of folding and assembly of the human chorionic gonadotropin alpha beta dimer by protein disulfide isomerase, *J. Biol. Chem. 268*, 16472−16482.
20. Muller, Y. A., Christinger, H. W., Keyt, B. A., and de Vos, A. M. (1997) The crystal structure of vascular endothelial growth factor (VEGF) refined to 1.93 Å resolution: multiple copy flexibility and receptor binding, *Structure 5*, 1325−1338.
21. Bedows, E., Norton, S. E., Huth, J. R., Suganuma, N., Boime, I., and Ruddon, R. W. (1994) Misfolded human chorionic gonadotropin beta subunits are secreted from transfected Chinese hamster ovary cells, *J. Biol. Chem. 269*, 10574−10580.
22. Feng, W., Bedows, E., Norton, S. E., and Ruddon, R. W. (1996) Novel covalent chaperone complexes associated with human chorionic gonadotropin beta subunit folding intermediates, *J. Biol. Chem. 271*, 18543−18548.

23. Feng, W., Matzuk, M. M., Mountjoy, K., Bedows, E., Ruddon, R. W., and Boime, I. (1995) The asparagine-linked oligosaccharides of the human chorionic gonadotropin beta subunit facilitate correct disulfide bond pairing, *J. Biol. Chem. 270*, 11851−11859.
24. Ruddon, R. W., Sherman, S. A., and Bedows, E. (1996) Protein folding in the endoplasmic reticulum: lessons from the human chorionic gonadotropin beta subunit, *Protein Sci. 5*, 1443−1452.
25. Gangani, R. A., Silva, D., Sherman, S. A., Perini, F., Bedows, E., and Keiderling, T. A. (2000) Folding studies on the human chorionic gonadotropin beta-subunit using optical spectroscopy of peptide fragments, *J. Am. Chem. Soc. 122*, 8623−8630.
26. Weissman, J. S., and Kim, P. S. (1992) Kinetic role of nonnative species in the folding of bovine pancreatic trypsin inhibitor, *Proc. Natl. Acad. Sci. U.S.A. 89*, 9900−9904.
27. Creighton, T. E. (1978) Experimental studies of protein folding and unfolding, *Prog. Biophys. Mol. Biol. 33*, 231−297.
28. Kim, P. S., and Baldwin, R. L. (1990) Intermediates in the folding reactions of small proteins, *Annu. Rev. Biochem. 59*, 631−660.
29. Ruddon, R. W., and Bedows, E. (1997) Assisted protein folding, *J. Biol. Chem. 272*, 3125−3128.

BI049856X